NOTES AND CORRESPONDENCE

Distribution of Helicity, CAPE, and Shear in Tropical Cyclones

JOHN MOLINARI AND DAVID VOLLARO

Department of Atmospheric and Environmental Sciences, University at Albany,
State University of New York, Albany, New York

(Manuscript received 30 January 2009, in final form 24 July 2009)

ABSTRACT

The previous study of helicity, CAPE, and shear in Hurricane Bonnie (1998) was extended to all eight tropical cyclones sampled by NASA during the Convection and Moisture Experiments (CAMEX). Storms were categorized as having large or small ambient vertical wind shear, with 10 m s^{-1} as the dividing line. In strongly sheared storms, the downshear mean helicity exceeded the upshear mean by a factor of 4. As in the previous study, the helicity differences resulted directly from the tropical cyclone response to ambient shear, with enhanced in-up-out flow and veering of the wind with height present downshear. CAPE in strongly sheared storms was 60% larger downshear. Mean inflow near the surface and the depth of the inflow layer each were 4 times larger downshear. At more than 30% of observation points outside the 100-km radius in the downshear right quadrant, midlatitude empirical parameters indicated a strong likelihood of supercells. No such points existed upshear in highly sheared storms. Much smaller upshear–downshear differences and little likelihood of severe cells occurred in storms with ambient wind shear below 10 m s^{-1}. In addition to these azimuthal asymmetries, highly sheared storms produced 30% larger area-averaged CAPE and double the area-averaged helicity versus relatively unsheared storms. The vortex-scale increase in these quantities lessens the negative impact of large vertical wind shear.

1. Introduction

Molinari and Vollaro (2008, hereafter MV08) examined the spatial variation of helicity and convective available potential energy (CAPE) in Hurricane Bonnie (1998). They made use of dropsonde data collected during the Third and Fourth Convection and Moisture Experiments (CAMEX-3 and CAMEX-4; Kakar et al. 2006) by the National Aeronautics and Space Administration (NASA). An enormous azimuthal variation of helicity over the lowest 3 and 6 km existed with respect to the direction of the ambient vertical wind shear. Mean helicity downshear of the center exceeded that upshear by a factor of 3. Mean CAPE downshear was also 3 times larger. The largest local helicity values, surpassing those associated with tornadic supercells in the middle latitudes, occurred in four sondes nearest to intense convective cells

in the hurricane. These cells had the spatial and temporal scales of supercells. The cells developed downshear, intensified as they moved to the left of the ambient shear, and decayed upshear. In the absence of sufficient radar, the presence of supercells could not be confirmed. Nevertheless, midlatitude empirical parameters exceeded supercell thresholds as a result of exceptional helicity combined with modest but sufficient CAPE. MV08 argued that the presence of the intense cells might have helped the storm maintain its intensity during a 36-h period in which ambient 850–200-hPa vertical shear remained near 12.5 m s^{-1}.

The large azimuthal variation of helicity in Hurricane Bonnie came about from differences in radial velocity arising from the tropical cyclone (TC) response to the ambient shear. Downshear this resulted in enhanced in–up–out flow that created strong turning of the wind with height and large helicity. Upshear, the ambient shear-induced circulation opposed the normal radial–vertical flow of the hurricane, producing much smaller helicity.

This note will extend the Hurricane Bonnie results to all tropical cyclones sampled by NASA during the

Corresponding author address: John Molinari, Dept. of Atmospheric and Environmental Sciences, ES-225, University at Albany/SUNY, Albany, NY 12222.
E-mail: molinari@atmos.albany.edu

CAMEX experiments. The additional data will reveal the sensitivity of these results to the magnitude of the ambient shear. The spatial distribution of helicity, CAPE, vertical wind shear, and empirical severe weather parameters in tropical cyclones will be shown.

2. Role of individual cells in tropical cyclones

Hendricks et al. (2004) and Montgomery et al. (2006) argued in their numerical simulations for the importance of "vortical" hot towers (VHTs), in which updrafts and rotation were coincident. They argued that VHTs were the preferred mode of convection in tropical cyclones. These cells lasted about an hour and gained their rotation from the tilting of horizontal vorticity in the vortex and vertical stretching. Hendricks et al. (2004) argued for an upscale vorticity cascade to the tropical storm scale via mergers and axisymmetrization of these VHTs. The VHTs also played a critical role in the thermodynamics of the tropical cyclones by moistening the midtroposphere. Montgomery et al. (2006) provide a full discussion of how these concepts fit with those proposed previously in the literature.

VHTs are helical by definition because they contain coincident updrafts and vertical vorticity. Levich and Tzvetkov (1984) noted that mean-square helicity tends to organize itself on larger scales, somewhat analogous to an upscale energy cascade (Lilly 1986). Levina (2006) and Levina and Burylov (2006) noted a positive feedback between tangential flow and radial flow in a vortex as a result of a parameterized source of helicity from small-scale convective cells. Thus, both VHTs and helicity-based arguments provide a similar dynamical framework.

Supercells represent an extreme example of helical cells. They typically last 90 min or more and are comprised of quasi-steady rotating updrafts. They develop in the presence of large vertical wind shear. They are characterized by large vorticity (on the order of 10^{-2} s^{-1}) in midlevels arising from the tilting of horizontal vorticity. The dynamics of supercells is described by Weisman and Rotunno (2000) and references therein. It is apparent that VHTs and supercells have some characteristics in common.

Davies-Jones et al. (1990) developed an empirical parameter for predicting the possibility of supercell occurrence using soundings. It made use of the vertical integral of cell-relative helicity (simply "helicity" hereafter), given by

$$\text{SREH} = \int_0^h \left[(\mathbf{v} - \mathbf{c}) \cdot \left(\mathbf{k} \times \frac{\partial \mathbf{v}}{\partial z} \right) \right] dz, \qquad (1)$$

where $\mathbf{c}$ represents the cell motion vector and h is the layer depth, often taken as 3 km. Because convective

cells are influenced by the local wind and helicity, $\mathbf{v}$ represents the measured wind vector, not the wind with respect to the movement of the hurricane center.

The cylindrical coordinate form for total (not cell-relative) helicity (e.g., Yamei and Rongsheng 2003; MV08) is given by

$$H_{\text{TOT}} = -v_r \frac{\partial v_\lambda}{\partial z} + v_\lambda \frac{\partial v_r}{\partial z}, \qquad (2)$$

where v_r and v_λ and are the radial and tangential velocity components, respectively. Following the arguments of MV08, the vertical term in the helicity expression has been neglected in Eq. (2). Because tangential velocity is always large in the lower troposphere in tropical cyclones, a strong upward increase in radial velocity would create large values of total helicity in tropical cyclones. MV08 showed that this reasoning extended to cell-relative helicity as well.

The use of helicity theory (Davies-Jones 1984) as a basis for understanding supercell evolution has been questioned by Weisman and Rotunno (2000). They noted two weaknesses of this theory: (i) it requires specification of cell motion and assumption of cell steadiness, whereas in fact these processes are an integral part of the overall dynamics, and (ii) the theory is quasi-linear, and the neglected nonlinear terms are sometimes significant. These issues should not limit the value of helicity in this study for the following reasons:

1) Weisman and Rotunno (2000) noted that the helicity theory worked best for curved hodographs, which dominate the hodograph structure in tropical cyclones (McCaul 1991; MV08).

2) Helicity is used in this study not to understand how the cells themselves evolve, but rather as a scalar marker indicating the probability of supercell occurrence. Numerous papers have verified the value of helicity for such purposes in middle latitudes (e.g., Brandes et al. 1988; Davies-Jones et al. 1990; Johns and Doswell 1992; Kerr and Darkow 1996; Thompson et al. 2003).

3) It has been hypothesized that large-helicity cells effectively resist dissipation (Lilly 1986). Although this has not been proven, such cells contain large local values of vertical vorticity, which allows them to resist distortion as a result of inertial stability and Rossby elasticity (e.g., Reasor et al. 2004). Considerable support exists for helicity providing a marker for cell lifetime, based on the empirical studies noted in item 2 above and in the numerical simulations of Droegemeier et al. (1993).

McCaul (1987, 1991) showed elevated values of helicity in the vicinity of tornadic supercells associated with

TABLE 1. Dropsondes used in this study; TS, H, and TS/H refer to whether the sondes were released in a given storm at tropical storm or hurricane strength, or both.

Storm	TS/H	Number of sondes	Large ambient shear ≥ 10 m s^{-1}	Small ambient shear <10 m s^{-1}
Bonnie 1998	H	17	9	8
Danielle 1998	H	28	0	28
Earl 1998	H	2	2	0
Georges 1998	H	6	0	6
Chantal 2001	TS	5	5	0
Erin 2001	H	9	0	9
Gabrielle 2001	TS/H	10	10	0
Humberto 2001	TS/H	35	32	3
Total 1998/2001		112	58	54

hurricanes after landfall. McCaul and Weisman (1996) simulated supercell formation using characteristic soundings after tropical cyclone landfall. The resultant supercells resembled those in middle latitude severe convection but had smaller vertical extent, consistent with shallower layers of vertical wind shear and CAPE. The large helicity in the soundings of McCaul (1991) arose from strong low-level shear associated both with frictional decay after landfall and with baroclinicity. Such circumstances are much less likely over water. The current note will not consider shallow supercells typical of hurricane landfall environments, which are well understood as a result of the work of McCaul and Weisman (1996, 2001) and various other papers since. The cells of interest in this note are deep cells in tropical cyclones over open ocean. They are supported by local vertical shear maxima that arise not from the landfall process but rather from the response of the tropical cyclone to large ambient vertical wind shear.

3. Data sources and calculation methods

Cell motion in Eq. (1) will be estimated using the method of Ramsay and Doswell (2005). This estimate combines a mean wind with a vertical shear–induced deflection from the mean wind, consistent with the motion of supercells. Only a few studies have examined the motion of individual cells in tropical cyclones. Barnes et al. (1991) and Powell (1990) found that cells in hurricane rainbands moved fairly close to the mean wind over 6 km, similar to ordinary convection in middle latitudes. Black et al. (2002) and Eastin et al. (2005) found cells that moved more slowly than the wind, consistent both with vortex Rossby waves (Montgomery and Kallenbach 1997) and with supercells (MV08). Spratt et al. (1997) found supercell-like motion in cells over land before tropical cyclone landfall. To the extent that cells move with the mean wind, McCaul (1991) and MV08 have shown a 40% reduction in helicity estimates versus the Ramsay and Doswell (2005) method. Nev-

ertheless, MV08 showed that regardless of the choice of five cell motion estimates they tested, every calculation showed the same helicity distribution with respect to ambient vertical wind shear, and all produced extreme values of helicity near intense cells.

Similar to MV08, sondes were not used for helicity calculations if wind data were missing in a layer at the surface of 200 m or more or were missing over more than a 1.5-km layer anywhere else in the lowest 8 km. The surface layer criterion was needed because one aspect of cell motion calculations required mean wind over the lowest 500 m. CAPE calculations used the same criteria, except that up to a 2-km layer of missing temperature and dewpoint was allowed. All but two of the sondes used for helicity calculations were suitable for CAPE as well. All variables were interpolated with height to 100 m levels.

After removal of soundings with missing data, 112 dropsondes remained within 400 km of the center of eight tropical cyclones sampled during CAMEX-3 and CAMEX-4 (Kakar et al. 2006). Five storms were hurricanes, one was a tropical storm, and two were sampled at both stages. Table 1 describes the sonde distribution. All but six were released from a DC-8 aircraft flying near the 250-hPa level; the others were released from an ER-2 aircraft located near 70 hPa. Similar numbers of sondes were released during periods of relatively small ambient vertical wind shear (<10 m s^{-1}) and during large ambient shear. More than half the sondes represent only two storms, Humberto and Danielle. This should not distort the results, however, because the azimuthal helicity variation noted in MV08 was present in every strongly sheared storm. All but 11 of the sondes were released in tropical cyclones with centers north of 20° latitude. The results of this note may not hold for storms in the deep tropics.

MV08 did not include a correction for sonde drift. Such drift could have a significant influence on the calculation of helicity in tropical cyclones. A vortex with constant, purely tangential cyclonic wind at all levels

contains zero total helicity according to Eq. (2). A sonde that moves 90° of azimuth (which could occur near the eyewall) but has all winds plotted at the release point will show an apparent clockwise turning of wind with height (i.e., positive helicity). In reality this turning reflects the curvature of the horizontal wind. This error can be prevented by working with radial and tangential velocity rather than Cartesian wind components. The previous example then produces a constant tangential velocity with height and, as appropriate, zero helicity. This procedure for incorporating sonde drift was used for all data in this study. When it was applied to data from MV08, helicity was reduced by 5%–8% outside of the 75-km radius. Within that radius, large azimuthal displacements of the sondes sometimes occurred. This creates uncertainty in the helicity calculation even with the correction above because the sondes do not represent a single column when displacement is large. As a result, helicity and CAPE in this study will be shown only beyond the 75-km radius. This decision eliminated 12 inner-core sondes and reduced the total to 100.

CAPE in this study is calculated using the virtual temperature difference between a parcel lifted pseudo-adiabatically and the dropsonde sounding after mixing the parcel through a 500-m depth centered on its level of origin. The maximum CAPE from any level below 3 km was chosen. In all but three soundings the maximum CAPE arose from a parcel originating within the lowest kilometer.

Two issues arose in the calculation of CAPE. Most sondes were released from near the 250-hPa level. Any CAPE above the release level would be missed if only the dropsonde soundings were used. This potential problem was addressed by a two-step process: (i) assigning temperature values using gridded analyses from the European Centre for Medium-Range Weather Forecasts (ECMWF) above the dropsonde release point, interpolated from the model grid to the release point location; and (ii) adjusting the ECMWF values at all levels by a constant equal to the difference between the interpolated ECMWF value and the dropsonde value at their first common level. The second step resembles that used by Bogner et al. (2000). MV08 used the first step but not the second, which then required additional procedures for correcting discontinuities. The current procedure better prevents under- or overestimates of CAPE caused solely by differences in the ECMWF temperatures from those observed by the sonde.

The second issue in the CAPE calculation involved the error described by Bogner et al. (2000) regarding unrealistically large relative humidity in well-mixed layers near the surface. It appears to relate to the hygristor remaining wet after passage through a low cloud
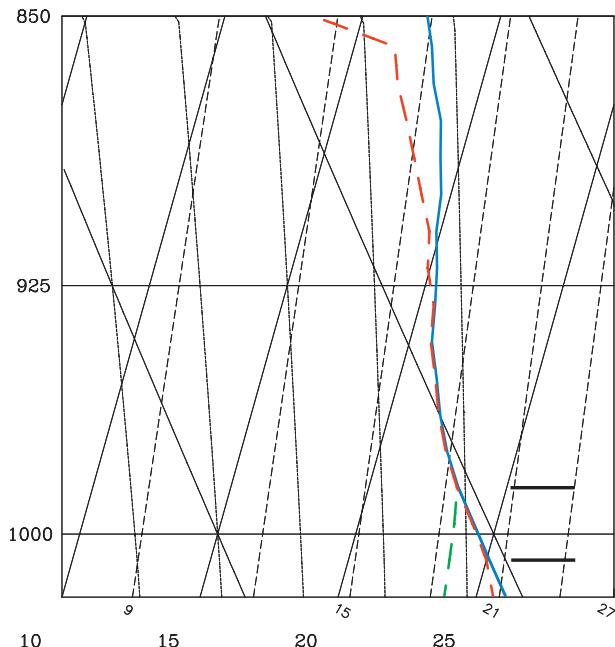

FIG. 1. Example of the Bogner et al. (2000) correction for erroneous boundary layer moisture for a sounding taken in Hurricane Erin (2001). Shown are temperature (blue solid), dewpoint (red dashed), and modified dewpoint (green dashed). The bracketed layer meets the criteria for the correction: relative humidity >98% and lapse rate >8 K km^{-1}.

during its descent. Barnes (2008; see his Fig. 5) suggested that 25% of the GPS sondes in his study contained this error. To address the problem, we will use the method of Bogner et al. (2000). This method replaces the erroneous mixing ratio by assuming it is well mixed through a layer starting 10 hPa above the top of the well-mixed layer in potential temperature. The correction was applied only if a layer existed between 900 hPa and the surface that contained relative humidity above 98% and a temperature lapse rate greater than 8 K km^{-1} (81% of the dry adiabatic rate). Overall, 9% of soundings required this correction.

Figure 1 gives an example from Hurricane Erin (2001), showing the layer meeting the two criteria, the original sounding, and the modified dewpoint profile produced by the correction. In the sounding shown, CAPE was reduced from 2190 to 1760 J kg^{-1}. For soundings with this error, the reduced CAPE values are almost certainly more realistic than the original.

As in MV08, two calculations of vertical wind shear are relevant. Ambient vertical wind shear from 850 to 200 hPa was calculated from 1.125° gridded ECMWF analyses over 500 km of radius (Corbosiero and Molinari 2002). The local (single-column) vertical wind shear will be taken as the vector difference between the 5500–6000-m mean wind and the 0–500-m mean wind. The
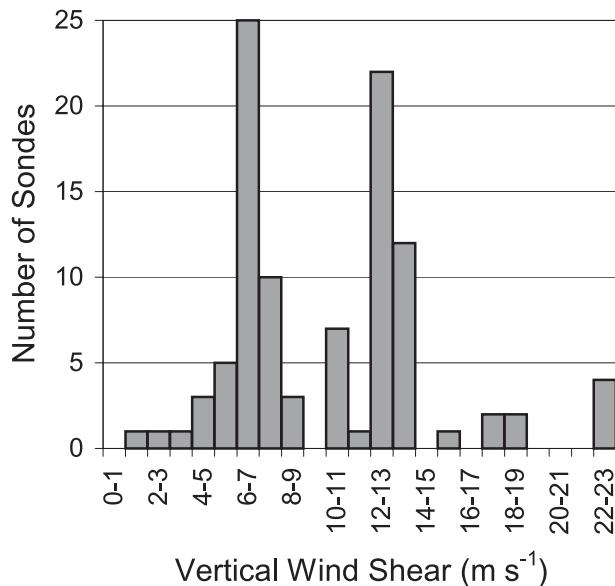
FIG. 2. Number of dropsondes in each 1 m s^{-1} range of ambient vertical wind shear.

terms "upshear" and "downshear" will always refer to the side of the storm with respect to the ambient shear vector. Following standard practice in tropical meteorology research, vertical wind shear will be expressed in m s^{-1} for each layer. Using mean pressure heights from the hurricane season sounding of Jordan (1958), 10 m s^{-1} of 850–200-hPa ambient shear is equivalent to shear of 0.92×10^{-3} s^{-1}, or roughly 1 m s^{-1} km^{-1}.

Ambient shear was calculated for each 6-h period centered on 0000, 0600, 1200, and 1800 UTC. Each sonde was labeled according to the ambient shear magnitude at the time of its release. Figure 2 shows the distribution of the number of dropsondes with respect to the magnitude of the ambient shear. The dividing line between small and large ambient shear was chosen as 10 m s^{-1} in part because of the break in the distribution. The mean (10.0 m s^{-1}) and median (10.4 m s^{-1}) shear values also support the same dividing line. No clear dynamical significance is attached to this threshold, except to note that upshear–downshear differences were much larger when ambient shear exceeded the threshold. When an 8 m s^{-1} threshold was chosen, only three

sondes were shifted from small to large ambient shear, and the results were virtually identical.

4. Results

a. Helicity and local vertical wind shear

Table 2 shows upshear and downshear mean helicity for both large and small values of ambient wind shear. For highly sheared tropical cyclones, mean helicity downshear exceeded its value upshear by more than a factor of 4. The downshear mean of 200 m^2 s^{-2} compared favorably to values in midlatitude supercell environments (100–240 m^2 s^{-2}; Houston and Wilhelmson 2007). When ambient shear was small, downshear helicity still exceeded that upshear, but by a smaller margin, and the mean helicity did not reach values suggestive of supercells in either region.

Table 2 also shows analogous variations for 0–6-km local vertical wind shear magnitude. Its mean always fell below 10 m s^{-1} except downshear of the center of storms with large ambient shear. Thompson et al. (2003) noted that the probability of supercells in middle latitudes grows dramatically as 0–6-km vertical wind shear rises from 15 to 20 m s^{-1}. The mean value of nearly 18 m s^{-1} downshear of storms with large ambient shear again provides potential support for supercells in that region, but nowhere else.

Unexpectedly, the area-averaged helicity (i.e., averaging all sondes, both upshear and downshear) in highly sheared storms reached more than double the value of storms with smaller ambient shear (130 versus 58 m^2 s^{-2}). The reasons for this are not certain. The growth in helicity is consistent with the increase in vertical mass flux with the magnitude of ambient shear in hurricanes found by Davis et al. (2008).

Figure 3 shows the locations of each dropsonde with respect to the storm centers, rotated with respect to the ambient wind shear following Corbosiero and Molinari (2002). Downshear lies to the right. Red circles indicate helicity above 100 m^2 s^{-2}, with size proportional to helicity. When ambient shear was small (Fig. 3a), only a handful of points had large helicity, with most falling in the downshear right quadrant. For highly sheared storms (Fig. 3b), large helicity, including several points

TABLE 2. Helicity [0–3 km, from text Eq. (1)] and 0–6-km local vertical wind shear magnitude, each averaged over all upshear and all downshear dropsondes, for both small and large ambient vertical wind shear.

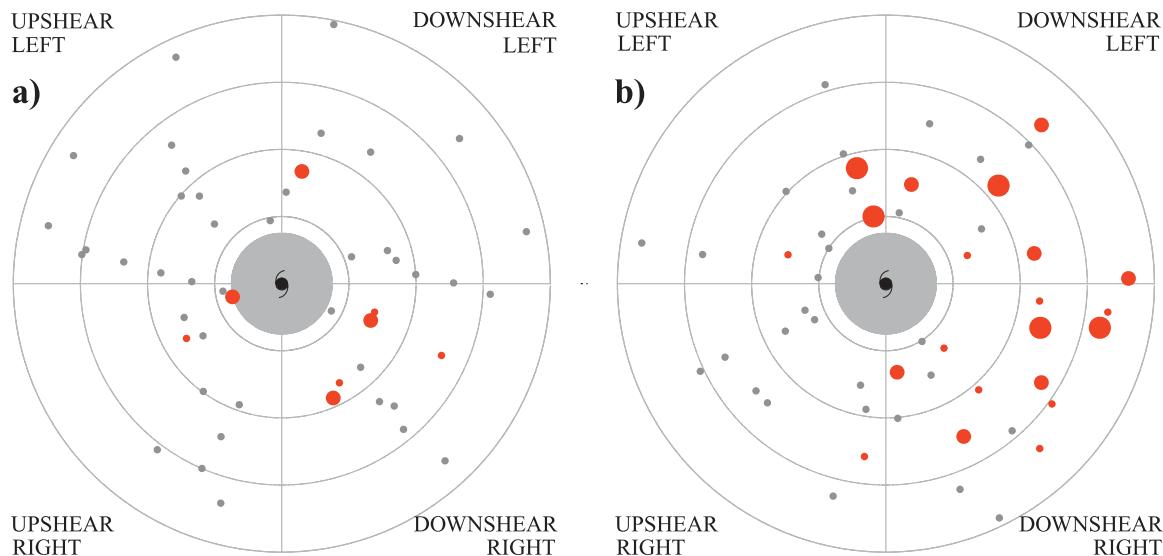| Variable	Low ambient shear <10 m s^{-1}		High ambient shear ≥10 m s^{-1}	
	Upshear mean	Downshear mean	Upshear mean	Downshear mean
Helicity (m^2 s^{-2})	49	69	44	200
0–6-km local vertical wind shear (m s^{-1})	7.0	9.3	8.1	17.7

FIG. 3. Location of dropsondes and 0–3-km helicity values for (a) small ambient vertical wind shear and (b) large ambient shear. Dropsonde locations have been positioned with respect to the moving center at the time of their splashdown and have been rotated with respect to the ambient vertical wind shear following Corbosiero and Molinari (2002). The right half represents downshear. Range circles are shown every 100 km. Gray dots represent helicity <100 m^2 s^{-2}; small red dots 100 m^2 s^{-2} $\leq$ SREH $<$ 200 m^2 s^{-2}; medium red dots 200 m^2 s^{-2} $\leq$ SREH $<$ 300 m^2 s^{-2}; large red dots $\geq$300 m^2 s^{-2}. Helicity was not calculated within 75 km of the center (shaded) because of potential errors associated with sonde drift.

above 300 m^2 s^{-2}, extended throughout the downshear region. Only one point exceeded 100 m^2 s^{-2} directly upshear.

Figure 4 shows the radial distribution of helicity for small and large ambient shear. For small ambient shear, helicity was slightly larger downshear, but mean values remained below 100 m^2 s^{-2}. For strongly sheared storms, the upshear–downshear differences amounted to almost an order of magnitude outside the 200-km radius.

Figure 5 shows mean radial velocity upshear and downshear, averaged over radii of 75–400 km, for both small (Fig. 5a) and large (Fig. 5b) ambient shear. For the reasons given in section 2, the measured radial velocity (rather than that relative to the tropical cyclone motion) is shown. When ambient shear was small, upshear and downshear mean radial velocity showed only modest differences. For highly sheared storms, radial velocity increased upward from the surface (strong inflow) to the 6-km level (strong outflow) downshear of the center. Upshear of the center, radial velocity increased upward only in the boundary layer. As a result, mean inflow depth downshear exceeded that upshear by a factor of 4.

Figure 5 is suggestive of results shown previously. Schneider and Barnes (2005) showed maximum inflow depths in the northwest quadrant of Hurricane Bonnie (1998) when the storm was near landfall. Using the ambient vertical shear at that time shown by MV08, this deep

inflow occurred downshear left. Similarly, Sitkowski and Barnes (2009) showed maximum inflow depths exceeding 4 km, also downshear left, in Hurricane Guillermo (1997) during its period of rapid intensification.
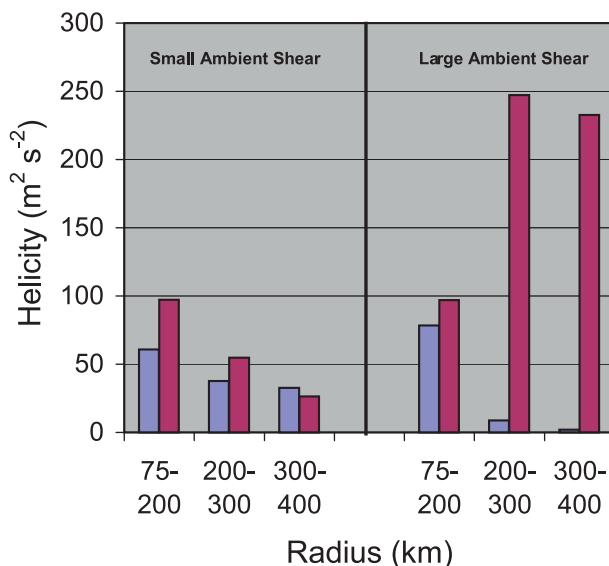

FIG. 4. Radial variation of 0–3-km helicity (m^2 s^{-2}) averaged over 75–200, 200–300, and 300–400 km for TCs experiencing (left) small and (right) large ambient shear. Upshear means are in blue and downshear in red.
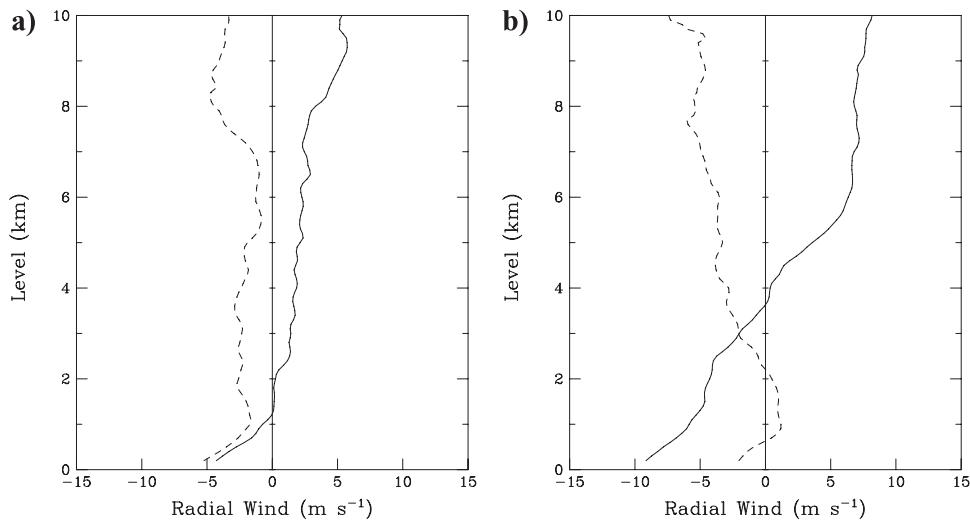
FIG. 5. Mean radial velocity (m s^{-1}) for downshear (solid) and upshear sondes (dashed) for TCs experiencing (a) small and (b) large ambient vertical wind shear. The $z = 0$ and $z = 100$-m levels are not shown because of insufficient observations.

Figure 6 shows the vertical profile of helicity upshear and downshear, again averaged over 75–400 km of radius, for small and large ambient shear. Helicity in Fig. 6 comes from a layer-by-layer calculation using Eq. (1). Consistent with Fig. 5, upshear and downshear profiles were similar for relatively unsheared tropical cyclones. Most of the helicity was present in the lowest kilometer, where frictional forcing produces a veering of wind with height. For highly sheared tropical cyclones the picture differed dramatically. Downshear the mean helicity exceeded 100 m^2 s^{-2} in the boundary layer alone. Substantial positive helicity existed throughout the lowest 6 km, the same layer over which Fig. 5 showed an upward increase of radial velocity. As a result, the cumulative differences in helicity between upshear and downshear grew with increasing h in Eq. (1), consistent with MV08.

b. CAPE and empirical severe weather parameters

Three empirical parameters used to predict severe weather in middle latitudes were considered. The energy–helicity parameter (EHI; see Davies 1993) represents a normalized product of helicity and CAPE; the supercell composite parameter (SCP; Thompson et al. 2002), a normalized product of helicity, CAPE, and bulk Richardson number shear (Weisman and Klemp 1986); and the vorticity generation parameter (VGP; Rasmussen and Blanchard 1998), the product of 0–6-km hodograph length
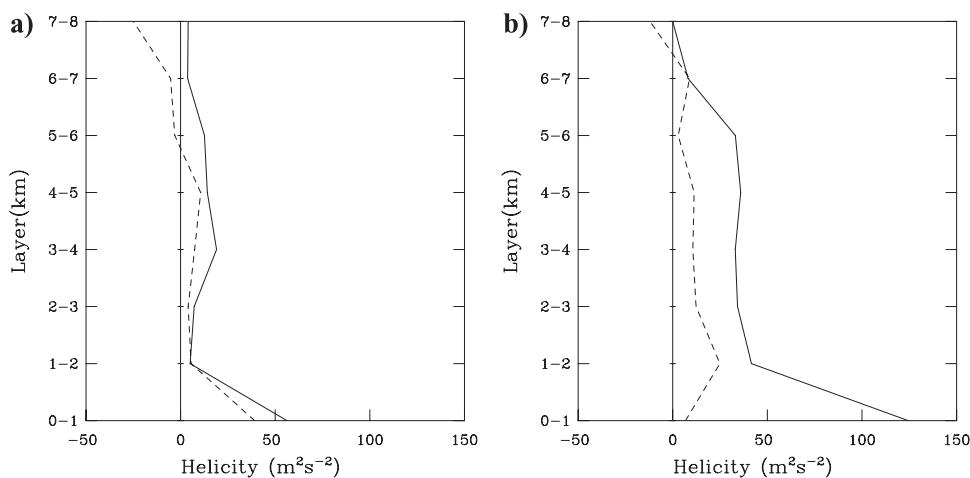

FIG. 6. Vertical profile of helicity (m^2 s^{-2}) in 1-km layers, averaged over upshear (dashed) and downshear (solid) soundings, for TCs experiencing (a) small and (b) large ambient wind shear.

TABLE 3. As in Table 2, but for CAPE, EHI (e.g., Davies 1993), SCP (Thompson et al. 2002), and VGP (Rasmussen and Blanchard 1998). The empirical parameters make use of "most unstable" CAPE (with no mixing through a layer before lifting the parcel). This estimate of CAPE is about 40% larger on average than the CAPE shown in this table. Median values in the vicinity of midlatitude supercells are taken from Rasmussen and Blanchard (1998). The exception is SCP, for which a threshold value is given following Thompson et al. (2002).

| Variable | Low ambient shear <10 m s^{-1} | | High ambient shear ≥ 10 m s^{-1} | | Middle latitude |
	Upshear mean	Downshear mean	Upshear mean	Downshear mean	Median supercell
CAPE (J kg^{-1})	720	690	700	1100	1150
EHI	0.27	0.40	0.06	1.70	0.64
SCP	0.05	0.13	0.02	1.01	1.00
VGP	0.11	0.13	0.08	0.21	0.21

and the square root of CAPE. The last of these provides a bulk measure of the tilting term in the vorticity equation and in effect substitutes vertical shear magnitude for helicity.

Thompson et al. (2002) argued that supercells were likely when SCP ≥ 1. Rasmussen and Blanchard (1998) found median values of EHI and VGP in supercell environments of 0.64 and 0.21, respectively. Hart and Korotky (1991) argued for the possibility of supercells when EHI > 1 and a strong likelihood when EHI > 2. These parameters were developed and refined using middle latitude data and thus cannot be blindly applied to the tropical cyclone, especially when considering the possibility of supercells. Nevertheless, it is reasonable to assume that severe localized cells become more likely as these parameter values increase.

Table 3 shows mean values in the same manner as Table 2, but for CAPE, EHI, SCP, and VGP. CAPE had similar means upshear and downshear in storms experiencing small ambient shear. In highly sheared storms, however, mean CAPE was nearly 60% larger downshear. This difference arose largely as a result of lower midlevel temperatures downshear (not shown). This temperature difference, like that for helicity, is likely brought about by the anomalies in vertical motion (rising motion downshear and subsidence upshear) forced by the ambient shear. Consistent with CAPE and helicity variations, the mean values of the empirical parameters in Table 3 exceeded those needed for supercells only downshear and only in highly sheared tropical cyclones. VGP, which does not use helicity, contained as strong a signal as the helicity-based measures. This suggests that the quantitative sensitivity of helicity to assumed cell motion is not distorting the results.

The overall mean CAPE in highly sheared tropical cyclones exceeded its value in relatively unsheared storms by almost 30% (910 versus 705 J kg^{-1}). As a result, large vertical wind shear produced not only azimuthal stability variations but also smaller overall convective stability and (see section 4a) larger helicity. In principle,

this provides an environment for stronger overall convection in a storm when ambient shear is larger.

Figure 7 shows the spatial distribution of EHI for large and small ambient shear. For highly sheared tropical cyclones, supercell criteria were met most often in the downshear right quadrant, for which 81% of dropsondes exceeded the median EHI criterion (Rasmussen and Blanchard 1998) and more than 30% indicated a strong likelihood of supercells using a midlatitude criterion (EHI > 2; Hart and Korotky 1991). For storms with small ambient shear, few points met the median criterion and none met the strong likelihood criterion.

A comparison of Figs. 3 and 7 shows that two left-of-ambient-shear soundings in strongly sheared hurricanes contained large helicity but did not meet the supercell criterion. CAPE fell below 500 J kg^{-1} at both points. In general, CAPE took on small values left of ambient shear. This shifted the most favorable region for supercells to directly downshear and downshear right, where both CAPE and helicity were sufficiently large.

Asymmetries in SCP and VGP resembled those in Fig. 7 (not shown). The azimuthal distribution was most dramatic for SCP. For storms experiencing small ambient shear, no points in any part of the storms met the supercell criterion. For highly sheared storms, soundings meeting the SCP threshold occurred only downshear of the center.

5. Discussion

MV08 argued for the following sequence of events: (i) ambient shear increases in a tropical cyclone; (ii) in–up–out flow is enhanced downshear and reduced upshear; (iii) as a direct result, helicity and CAPE increase downshear; and (iv) convective cells, already favored downshear, become stronger and longer-lived as a result of the larger helicity and CAPE. The question then arises: what is the subsequent impact of these cells on vortex resilience to shear and on storm intensity? Because this study made use of data scattered over eight
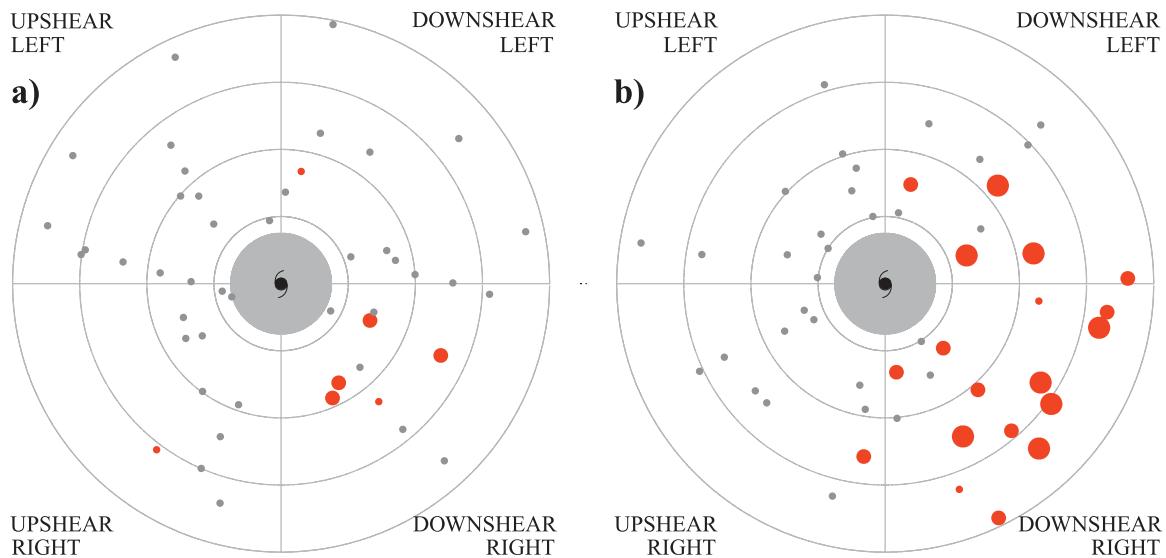
FIG. 7. As in Fig. 3, but showing EHI, for TCs experiencing (a) small and (b) large ambient shear. Gray dots represent EHI < 0.6; small red dots $0.6 \leq$ EHI < 1.0; medium red dots $1.0 \leq$ EHI < 2.0; large red dots EHI ≥ 2.

different hurricanes, these fundamental dynamical questions can be addressed only indirectly.

Reasor et al. (2004) have described the role of the tilt mode in sheared tropical cyclones. This represents a discrete Rossby wave associated with the vertical tilt of the vortex. The decay of this mode reduces the tilt and contributes to the resistance of the vortex to vertical shear. This theory holds for dry vortices and does not require the presence of individual cells or even of a radial–vertical circulation. Schecter and Montgomery (2007) noted that this process is more effective in the presence of lower static stability in cloudy regions. In the current study mean CAPE was larger (and thus stability was smaller) in highly sheared storms, and this could contribute to more effective resistance to vertical wind shear.

As noted in section 2, VHTs and other helical cells contribute collectively to storm spinup (e.g., Hendricks et al. 2004). The results of this study show that strong cells are much more likely in sheared storms. The role of these cells in storm intensification remains uncertain, however, because the strongest convection is supported outside of the 100-km radius over only half the storm.

Despite these uncertainties, several unambiguous conclusions can be made in this study. Conditions that favor severe convective cells have been shown to occur far more often in strongly sheared tropical cyclones (ambient shear above 10 m s^{-1}) than in relatively unsheared storms. Half the 6-h periods in CAMEX storms contained large shear, indicating that such circumstances are not unusual. The asymmetries induced by the shear extended at least to the 400-km radius. The downshear half of highly sheared storms contained the

following properties, averaged from 75–400-km radius, versus those upshear:

- 4 times larger 0–3-km helicity (Table 2; Fig. 3),
- more than 10 times larger 0–3-km helicity outside the 200-km radius (Fig. 4),
- 12 times larger 0–1-km helicity (Fig. 6),
- twice the 0–6-km vertical wind shear (Table 2),
- 58% larger CAPE (Table 3),
- 4 times the near-surface inflow (Fig. 5),
- inflow over a layer 4 times as deep (Fig. 5), and
- empirical support for supercells at several points downshear and especially downshear right, but never upshear (Fig. 7).

The helicity and CAPE variations described above each arose as a result of enhanced in–up–out flow downshear of the tropical cyclone center, as well as suppressed radial–vertical flow upshear, in response to the ambient shear. Convective cells are known to be favored downshear in tropical cyclones (e.g., Black et al. 2002; Corbosiero and Molinari 2002). Black et al. (2002) attributed this to a shear-induced increase in convergence and upward motion downshear. The enhanced values of helicity, shear, and CAPE described in this paper also favor cell growth downshear.

In addition to the upshear–downshear anomalies described above, the area-averaged helicity and CAPE in the presence of large ambient shear exceeded those in storms with small ambient shear. This overall reduction in stability and increase in helicity might represent a positive influence of large vertical wind shear that could partially offset the greater ventilation of the storm core.

The empirical parameters used in this study support the possible existence of supercells in tropical cyclones, especially in the downshear right quadrant outside of the 100-km radius. Supercells have been observed in tropical cyclones after landfall (e.g., McCaul et al. 2004) and near land (Baker et al. 2009). Radar data are needed to confirm whether such cells occur in tropical cyclones over open ocean. Many questions about convection in tropical cyclones remain unanswered. What is the range of scales of organized convection and associated vorticity anomalies? What is the proportion of ordinary hot towers versus VHTs? To what extent is the vast middle latitude severe weather literature relevant to tropical cyclones? These questions have only begun to be addressed (e.g., Sippel et al. 2006; Eastin et al. 2005; Eastin and Link 2008; Smith and Eastin 2008). The structure, organization, and impact of convective cells in tropical cyclones remain a fruitful area for research.

REFERENCES

Baker, A. K., M. D. Parker, and M. D. Eastin, 2009: Environmental ingredients for supercells and tornadoes within Hurricane Ivan. *Wea. Forecasting,* **24,** 223–244.

Barnes, G. M., 2008: Atypical thermodynamic profiles in hurricanes. *Mon. Wea. Rev.,* **136,** 631–643.

——, J. F. Gamache, M. A. LeMone, and G. J. Stossmeister, 1991: A convective cell in a hurricane rainband. *Mon. Wea. Rev.,* **119,** 776–794.

Black, M. L., J. F. Gamache, F. D. Marks Jr., C. E. Samsury, and H. E. Willoughby, 2002: Eastern Pacific Hurricanes Jimena of 1991 and Olivia of 1994: The effect of vertical shear on structure and intensity. *Mon. Wea. Rev.,* **130,** 2291–2312.

Bogner, P. B., G. M. Barnes, and J. L. Franklin, 2000: Conditional instability and shear for six hurricanes over the Atlantic Ocean. *Wea. Forecasting,* **15,** 192–207.

Brandes, E. A., R. P. Davies-Jones, and B. C. Johnson, 1988: Streamwise vorticity effects on supercell morphology and persistence. *J. Atmos. Sci.,* **45,** 947–963.

Corbosiero, K. L., and J. Molinari, 2002: The effects of vertical wind shear on the distribution of convection in tropical cyclones. *Mon. Wea. Rev.,* **130,** 2110–2123.

Davies, J. M., 1993: Hourly helicity, instability, and EHI in forecasting supercell tornadoes. Preprints, *17th Conf. on Severe Local Storms,* Kansas City, MO, Amer. Meteor. Soc., 107–111.

Davies-Jones, R. P., 1984: Streamwise vorticity: The origin of updraft rotation in supercell storms. *J. Atmos. Sci.,* **41,** 2991–3006.

——, D. Burgess, and M. Foster, 1990: Test of helicity as a tornado forecast parameter. Preprints, *16th Conf. on Severe Local Storms,* Kanaskis, AB, Canada, Amer. Meteor. Soc., 588–592.

Davis, C. A., S. C. Jones, and M. Riemer, 2008: Hurricane vortex dynamics during Atlantic extratropical transition. *J. Atmos. Sci.,* **65,** 714–736.

Droegemeier, K. K., S. M. Lazarus, and R. P. Davies-Jones, 1993: The influence of helicity on numerically simulated convective storms. *Mon. Wea. Rev.,* **121,** 2005–2029.

Eastin, M. D., and M. C. Link, 2008: Mini-supercells observed in an offshore rainband of Hurricane Ivan (2004). Preprints, *28th Conf. on Hurricanes and Tropical Meteor.,* Orlando, FL, Amer. Meteor. Soc., 12C.1. [Available online at http://ams.confex.com/ams/28Hurricanes/techprogram/paper_137620.htm.]

——, W. M. Gray, and P. G. Black, 2005: Buoyancy of convective vertical motions in the inner core of intense hurricanes. Part II: Case studies. *Mon. Wea. Rev.,* **133,** 209–227.

Hart, J. A., and W. Korotky, 1991: The SHARP workstation v1.50 users' guide. National Weather Service, NOAA, U.S. Dept. Commerce, 30 pp. [Available from NWS Eastern Region Headquarters, 630 Johnson Ave., Bohemia, NY 11716.]

Hendricks, E. A., M. T. Montgomery, and C. A. Davis, 2004: The role of "vortical" hot towers in the formation of Tropical Cyclone Diana (1984). *J. Atmos. Sci.,* **61,** 1209–1232.

Houston, A. L., and R. B. Wilhelmson, 2007: Observational analysis of the 27 May 1997 central Texas tornadic event. Part I: Prestorm environment and storm maintenance/propagation. *Mon. Wea. Rev.,* **135,** 701–726.

Johns, R. H., and C. A. Doswell III, 1992: Severe local storms forecasting. *Wea. Forecasting,* **7,** 588–612.

Jordan, C. L., 1958: Mean soundings for the West Indies area. *J. Atmos. Sci.,* **15,** 91–97.

Kakar, R., M. Goodman, R. Hood, and A. Guillory, 2006: Overview of the Convection and Moisture Experiment (CAMEX). *J. Atmos. Sci.,* **63,** 5–18.

Kerr, B. W., and G. L. Darkow, 1996: Storm-relative winds and helicity in the tornadic thunderstorm environment. *Wea. Forecasting,* **11,** 489–505.

Levich, E., and E. Tzvetkov, 1984: Helical cyclogenesis. *Phys. Lett.,* **100A,** 53–56.

Levina, G. V., 2006: Parameterization of helical turbulence in numerical models of intense atmospheric vortices (trans. from Russian). *Doklady Earth Sci.,* **411A,** 1417–1421.

——, and I. A. Burylov, 2006: Numerical simulation of helical-vortex effects in Rayleigh–Benard convection. *Nonlinear Processes Geophys.,* **13,** 205–222.

Lilly, D. K., 1986: The structure, energetics, and propagation of rotating convective storms. Part II: Helicity and storm stabilization. *J. Atmos. Sci.,* **43,** 126–140.

McCaul, E. W., Jr., 1987: Observations of the Hurricane "Danny" tornado outbreak of 16 August 1985. *Mon. Wea. Rev.,* **115,** 1206–1223.

——, 1991: Buoyancy and shear characteristics of hurricane–tornado environments. *Mon. Wea. Rev.,* **119,** 1954–1978.

——, and M. L. Weisman, 1996: Simulations of shallow supercell storms in landfalling hurricane environments. *Mon. Wea. Rev.,* **124,** 408–429.

——, and ——, 2001: The sensitivity of simulated supercell structure and intensity to variations in the shapes of environmental buoyancy and shear profiles. *Mon. Wea. Rev.,* **129,** 664–687.

——, D. E. Buechler, S. J. Goodman, and M. Cammarata, 2004: Doppler radar and lightning network observations of a severe outbreak of tropical cyclone tornadoes. *Mon. Wea. Rev.,* **132,** 1747–1763.

Molinari, J., and D. Vollaro, 2008: Extreme helicity and intense convective towers in Hurricane Bonnie. *Mon. Wea. Rev.,* **136,** 4355–4372.

Montgomery, M. T., and R. J. Kallenbach, 1997: A theory for vortex Rossby waves and its application to spiral bands and intensity changes in hurricanes. *Quart. J. Roy. Meteor. Soc.,* **123,** 435–465.

——, M. E. Nicholls, T. A. Cram, and A. B. Saunders, 2006: A vortical hot tower route to tropical cyclogenesis. *J. Atmos. Sci.,* **63,** 355–386.

Powell, M. D., 1990: Boundary layer structure and dynamics in outer hurricane rainbands. Part I: Mesoscale rainfall and kinematic structure. *Mon. Wea. Rev.,* **118,** 891–917.

Ramsay, H. A., and C. A. Doswell, 2005: A sensitivity study of hodograph-based methods for estimating supercell motion. *Wea. Forecasting,* **20,** 954–970.

Rasmussen, E. N., and D. O. Blanchard, 1998: A baseline climatology of sounding-derived supercell and tornado forecast parameters. *Wea. Forecasting,* **13,** 1148–1164.

Reasor, P. D., M. T. Montgomery, and L. D. Grasso, 2004: A new look at the problem of tropical cyclones in vertical shear flow: Vortex resiliency. *J. Atmos. Sci.,* **61,** 3–22.

Schecter, D. A., and M. T. Montgomery, 2007: Waves in a cloudy vortex. *J. Atmos. Sci.,* **64,** 314–337.

Schneider, R., and G. M. Barnes, 2005: Low-level kinematic, thermodynamic, and reflectivity fields associated with Hurricane Bonnie (1998) at landfall. *Mon. Wea. Rev.,* **133,** 3243–3259.

Sippel, J. A., J. W. Nielsen-Gammon, and S. E. Allen, 2006: The multiple-vortex nature of tropical cyclogenesis. *Mon. Wea. Rev.,* **134,** 1796–1814.

Sitkowski, M., and G. M. Barnes, 2009: Low-level thermodynamic, kinematic, and reflectivity fields of Hurricane Guillermo (1997) during rapid intensification. *Mon. Wea. Rev.,* **137,** 645–663.

Smith, K. C., and M. D. Eastin, 2008: Vortical hot towers in a rapidly intensifying mature hurricane: Observations and implications. Preprints, *28th Conf. on Hurricanes and Tropical Meteorology,* Orlando, FL, Amer. Meteor. Soc., 15A.4. [Available online at http://ams.confex.com/ams/28Hurricanes/techprogram/paper_138308.htm.]

Spratt, S. M., D. W. Sharp, P. Welsh, A. Sandrik, F. Alsheimer, and C. Paxton, 1997: A WSR-88D assessment of tropical cyclone outer rainband tornadoes. *Wea. Forecasting,* **12,** 479–501.

Thompson, R. L., R. Edwards, and J. A. Hart, 2002: Evaluation and interpretation of the supercell composite and significant tornado parameters at the Storm Prediction Center. Preprints, *21st Conf. on Severe Local Storms,* San Antonio, TX, Amer. Meteor. Soc., J11–J14.

——, ——, ——, K. L. Elmore, and P. Markowski, 2003: Close proximity soundings within supercell environments obtained from the Rapid Update Cycle. *Wea. Forecasting,* **18,** 1243–1261.

Weisman, M. L., and J. B. Klemp, 1986: Characteristics of isolated convective storms. *Mesoscale Meteorology and Forecasting,* P. Ray, Ed., Amer. Meteor. Soc., 331–358.

——, and R. Rotunno, 2000: The use of vertical wind shear versus helicity in interpreting supercell dynamics. *J. Atmos. Sci.,* **57,** 1452–1472.

Yamei, X., and W. Rongsheng, 2003: The conservation of helicity in Hurricane Andrew (1992) and the formation of the spiral rainband. *Adv. Atmos. Sci.,* **20,** 940–950.